

Percolation and localization in the random fuse model

Phani Kumar V V Nukala¹, Srđan Šimunović¹ and Stefano Zapperi²

¹ Computer Science and Mathematics Division, Oak Ridge National Laboratory, Oak Ridge, TN 37831-6359, USA

² INFN UdR Roma 1 and SMC, Dipartimento di Fisica, Università 'La Sapienza', Piazzale Aldo Moro 2, 00185 Roma, Italy
E-mail: nukalapk@ornl.gov, simunovics@ornl.gov and zapperi@pil.phys.uniroma1.it

Received 4 May 2004

Accepted 4 August 2004

Published 11 August 2004

Online at stacks.iop.org/JSTAT/2004/P08001

doi:10.1088/1742-5468/2004/08/P08001

Abstract. We analyse damage nucleation and localization in the random fuse model with strong disorder using numerical simulations. In the initial stages of the fracture process, damage evolves in an uncorrelated manner, resembling percolation. Subsequently, as the damage starts to accumulate, current enhancement at the tips of the microcracks leads eventually to catastrophic failure. We study this behaviour, quantifying the deviations from percolation and discussing alternative scaling laws for damage. The analysis of damage profiles confirms that localization occurs abruptly, starting from a uniform damage landscape. Finally, we show that the cumulative damage distribution follows the normal distribution, suggesting that damage is uncorrelated on large length scales.

Keywords: fracture (theory)

Contents

1. Introduction	2
2. Model	3
3. The role of disorder	6
4. Damage and percolation	8
5. Damage localization	14
6. Scaling of the damage density	19
7. The failure probability distribution	20
8. Discussion	21
Acknowledgments	23
References	23

1. Introduction

Understanding the scaling properties of fracture in disordered media represents an intriguing theoretical problem with important implications for practical applications [1]. Experiments have shown that for several materials under different loading conditions, the fracture surface is rough and can be described in terms of self-affine scaling [2] with universal exponents [3]. Scaling is also observed in acoustic emission experiments, where the distribution of pulses decays as a power law over several decades. Experimental observations have been reported for several materials such as wood [4], cellular glass [5], concrete [6] and paper [7], but universality does not seem to hold. The experimental observation of power law behaviour suggests an interpretation in terms of critical phenomena and scaling theories, but a complete theoretical explanation has not been found. The statistical properties of fracture in disordered media are often studied with lattice models, describing the medium as a discrete set of elastic bonds with random failure thresholds [1]. These numerical simulations are used in estimating the roughness of the fracture surface, which is found to be self-affine [8]–[11], and the power law distribution of avalanche precursors [12]–[16]. While the results agree qualitatively with experiments, a quantitative comparison is not always satisfactory.

Apart from the comparison with experiments, an important theoretical issue is understanding the origin of the scaling behaviour observed in the numerical simulations of the lattice model. A very well studied model is the random fuse model (RFM), where a lattice of fuses with a random threshold are subject to an increasing voltage [21, 1, 13], [17]–[20]. A resistor network represents a scalar analogue of an elastic medium and is thus relatively simple to analyse, while retaining some important characteristic features of the problem.

Simulations of the RFM show that the type of behaviour at macroscopic fracture is significantly influenced by the amount of disorder [17]. When the disorder is narrowly

distributed, materials break down without significant precursors. As the disorder increases, substantial damage is accumulated prior to failure and the dynamics resembles percolation [22]. Indeed, in the limit of infinite disorder, the damage accumulation process can exactly be mapped onto a percolation problem [23]. It is still debated, however, whether percolation is applicable to the case of strong but non-infinite disorder. Recently, some evidence has been provided in this direction [24] suggesting that the critical exponent, ν , of the correlation length in the RFM with strong disorder is same as that of uncorrelated percolation (i.e. $\nu = 4/3$), and that the fuse model is in the same universality class of percolation. Close to failure, damage would then localize and the resulting crack roughness would ensue from a gradient percolation mechanism [24].

In the present work, we propose a different interpretation of damage localization in the RFM: while in the initial stages damage accumulates as in a percolation process, the final crack nucleates abruptly due to current enhancement, yielding the observed localization profiles. As a consequence of this, the damage localization length follows closely the scaling of the crack width. In addition, we test percolation scaling by simulating the RFM with triangular and diamond (a square lattice with bonds inclined at 45° to the bus bars) lattice topologies [21, 1] and different disorder distributions (uniform and power law). The numerical results allow us to exclude the possibility that $\nu = 4/3$, but could still be compatible with another value of ν , although deviations from scaling are observed for large sizes.

Finally, we show that the cumulative damage probability distribution at failure can be collapsed for different lattice sizes and follows the normal distribution. This suggests that damage is the sum of uncorrelated variables and thus no long-range correlations are present as would be expected in critical phenomena. This fact, together with the abrupt localization occurring right at failure, suggests the validity of the first-order transition hypothesis discussed in [13].

The paper is organized as follows. In section 2 we define the model and in section 3 we discuss the role of disorder. The percolation hypothesis is tested in section 4, while section 5 is devoted to damage localization. The scaling of the number of broken bonds is discussed in section 6. Section 7 presents the analysis of the failure probability distribution and section 8 briefly summarizes our conclusions.

2. Model

In the random thresholds fuse model, the lattice is initially fully intact with bonds having the same conductance, but the bond breaking thresholds, t , are randomly distributed on the basis of a thresholds probability distribution, $p(t)$. The burning of a fuse occurs irreversibly whenever the electrical current in the fuse exceeds the breaking threshold current value, t , of the fuse. Periodic boundary conditions are imposed in the horizontal direction to simulate an infinite system and a constant voltage difference, V , is applied between the top and the bottom of the lattice system bus bars.

Numerically, a unit voltage difference, $V = 1$, is set between the bus bars and the Kirchhoff equations are solved to determine the current flowing in each of the fuses. Subsequently, for each fuse j , the ratio between the current i_j and the breaking threshold t_j is evaluated, and the bond j_c having the largest value, $\max_j i_j/t_j$, is irreversibly removed (burnt). The current is redistributed instantaneously after a fuse is burnt, implying that

Table 1. A summary of the main results of the simulations for the uniform thresholds distribution, including the number of configurations used to average the results for each system size. p_p and p_f denote the mean fraction of broken bonds in a lattice system of size L at the peak load and at failure, respectively. Similarly, Δ_p and Δ_f denote the standard deviation of the fraction of broken bonds at the peak load and at failure respectively.

L	N_{config}	Triangular				Diamond			
		p_p	Δ_p	p_f	Δ_f	p_p	Δ_p	p_f	Δ_f
4	50 000	0.2070	0.0532	0.3030	0.0476	0.2367	0.0625	0.3611	0.0482
8	50 000	0.1813	0.0346	0.2440	0.0329	0.1794	0.0365	0.2576	0.0318
16	50 000	0.1612	0.0225	0.2023	0.0218	0.1470	0.0222	0.1972	0.0202
24	50 000	0.1513	0.0177	0.1841	0.0170	0.1340	0.0169	0.1731	0.0155
32	50 000	0.1451	0.0150	0.1731	0.0143	0.1267	0.0139	0.1596	0.0129
64	50 000	0.1325	0.0104	0.1524	0.0096	0.1132	0.0092	0.1353	0.0084
128	12 000	0.1222	0.0078	0.1362	0.0070	0.1031	0.0064	0.1181	0.0056
256	1 200	0.1142	0.0058	0.1238	0.0053	0.0955	0.0048	0.1052	0.0042
512	200	0.1072	0.0048	0.1136	0.0044				

Table 2. A summary of the main results of the simulations for the power law thresholds distribution, including the number of configurations used to average the results for each system size. p_p and p_f denote the mean fraction of broken bonds in a lattice system of size L at the peak load and at failure, respectively. Similarly, Δ_p and Δ_f denote the standard deviation of the fraction of broken bonds at the peak load and at failure respectively.

L	N_{config}	Triangular			
		p_p	Δ_p	p_f	Δ_f
4	50 000	0.5360	0.0450	0.5568	0.0437
8	50 000	0.5454	0.0324	0.5535	0.0318
16	50 000	0.5489	0.0217	0.5531	0.0213
24	50 000	0.5491	0.0170	0.5526	0.0166
32	50 000	0.5483	0.0143	0.5517	0.0139
64	25 000	0.5449	0.0096	0.5489	0.0092
128	1 400	0.5406	0.0082	0.5449	0.0080
256	32	0.5379	0.0045	0.5417	0.0040
512	10	0.5349	0.0037	0.5382	0.0032

the current relaxation in the lattice system is much faster than the breaking of a fuse. Each time a fuse is burnt, it is necessary to recalculate the current redistribution in the lattice to determine the subsequent breaking of a bond. The process of breaking bonds, one at a time, is repeated until the lattice system falls apart. In this work, we consider a uniform probability distribution, which is constant between 0 and 1, and a power law distribution $p(t) \propto t^{-1+\beta}$, $0 \leq t \leq 1$, with $\beta = 1/20$.

Numerical simulation of fracture using large fuse networks is often hampered due to the high computational cost associated with solving a new large set of linear equations every time a new lattice bond is broken. The authors have developed a rank-1 sparse

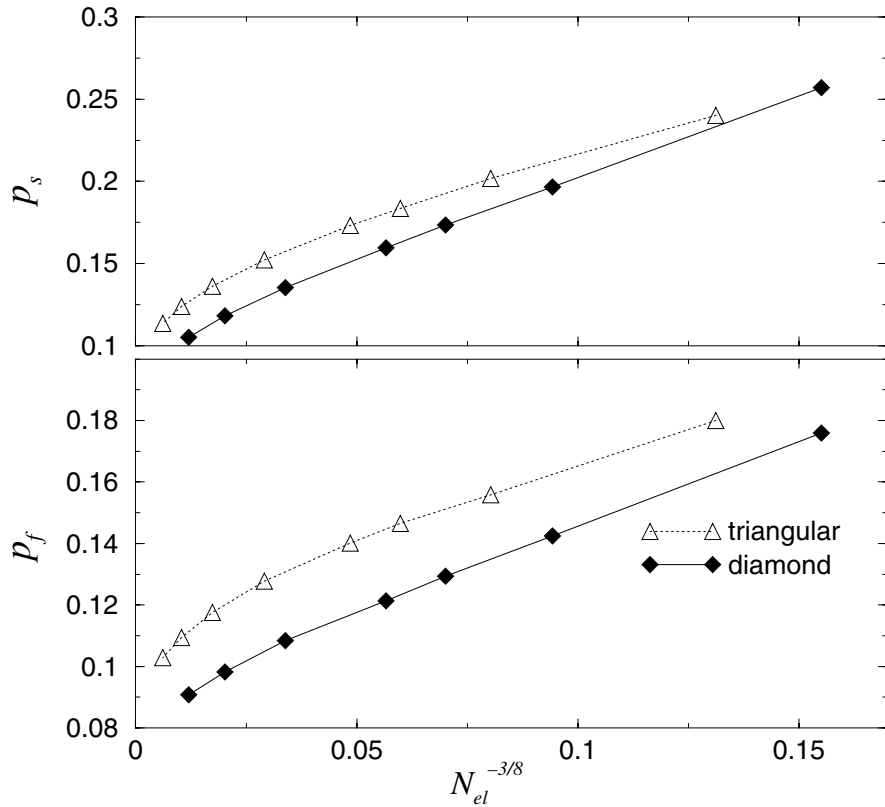


Figure 1. The 50% survival probability p_s (top) and the mean fraction of broken bonds p_f (bottom) plotted as a function of $N_{el}^{-3/8}$ for the uniform threshold distribution. If percolation scaling is obeyed, the data should follow a straight line. A net curvature is instead observed in all the data for large lattice sizes.

Cholesky factorization updating algorithm for simulating fracture using discrete lattice systems [20]. In comparison with the Fourier accelerated iterative schemes used for modelling lattice breakdown [28], this algorithm significantly reduced the computational time required for solving large lattice systems. Using this numerical algorithm, we were able to investigate damage evolution in larger lattice systems (e.g., for $L = 1024$), which to the authors' knowledge, is so far the largest lattice system used in studying damage evolution using initially fully intact discrete lattice systems. However, in this paper, we consider results up to $L = 512$ due to an insufficient number of sample configurations being available for $L = 1024$, which will be considered in a future publication.

Using the algorithm presented in [20], we have performed numerical simulations on two-dimensional triangular and diamond (a square lattice inclined at 45° between the bus bars) lattice networks. For many lattice system sizes, the numbers of sample configurations, N_{config} , used are excessively large to reduce the statistical error in the numerical results (see tables 1 and 2). Each numerical simulation was performed on a single processor of the *Eagle* (184 nodes with four 375 MHz Power3-II processors) supercomputer at the Oak Ridge National Laboratory. The N_{config} statistically independent configurations were simulated simultaneously on a number of processors available for computation.

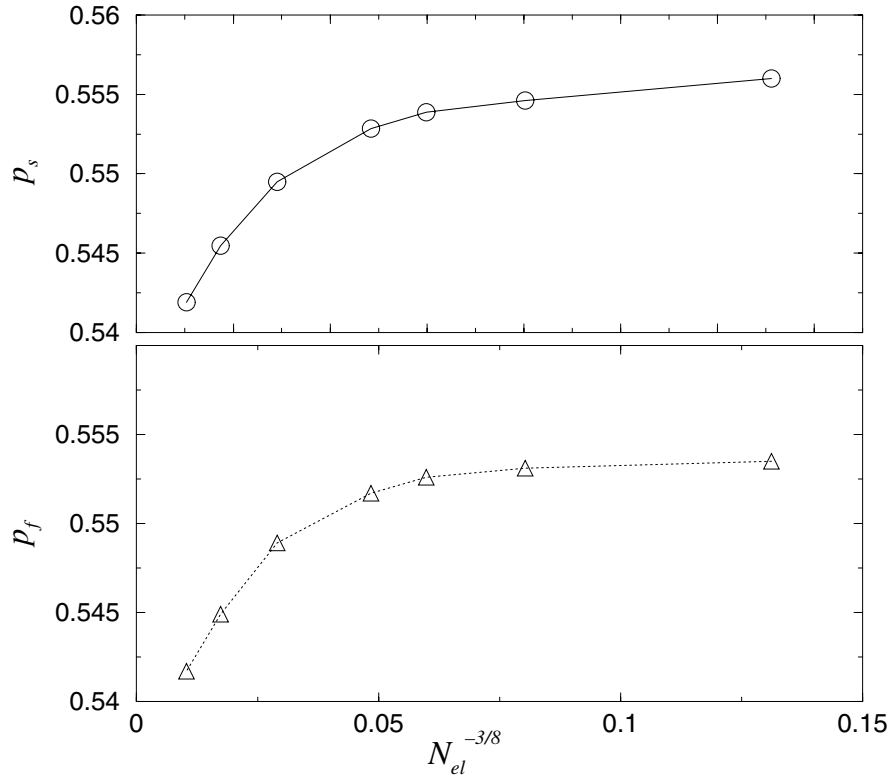


Figure 2. The 50% survival probability p_s and the mean fraction of broken bonds p_f plotted as a function of $N_{el}^{-3/8}$ for the power law threshold distribution. Percolation scaling is not obeyed.

3. The role of disorder

The disorder distribution clearly has an important effect on the fracture behaviour and a classification has been proposed in terms of a scale-invariant spectrum [29, 30], which for the uniform thresholds distribution ($0 \leq t \leq 1$) in terms of intensive variables, α_t and $f_t(\alpha_t)$, is given by [29, 30]

$$f_t(\alpha_t) = 2 - \alpha_t \quad \text{for } 0 \leq \alpha_t \leq 2 \quad (1)$$

where

$$\alpha_t = \frac{\log t}{\log L} \quad (2)$$

$$f_t(\alpha_t) = \frac{\log L^2 t p(t)}{\log L}. \quad (3)$$

Hence, for the uniform distribution between 0 and 1, the two control parameters ϕ_0 and ϕ_∞ that characterize the thresholds distribution $p(t)$ close to zero and infinity, respectively, are given by $\phi_0 = 1$ and $\phi_\infty = \infty$ [29, 30], where $\phi_{0/\infty}$ are defined by

$$\phi_{0/\infty} = \lim_{t \rightarrow 0/\infty} \left(\frac{\log(tp(t))}{\log(t)} \right). \quad (4)$$

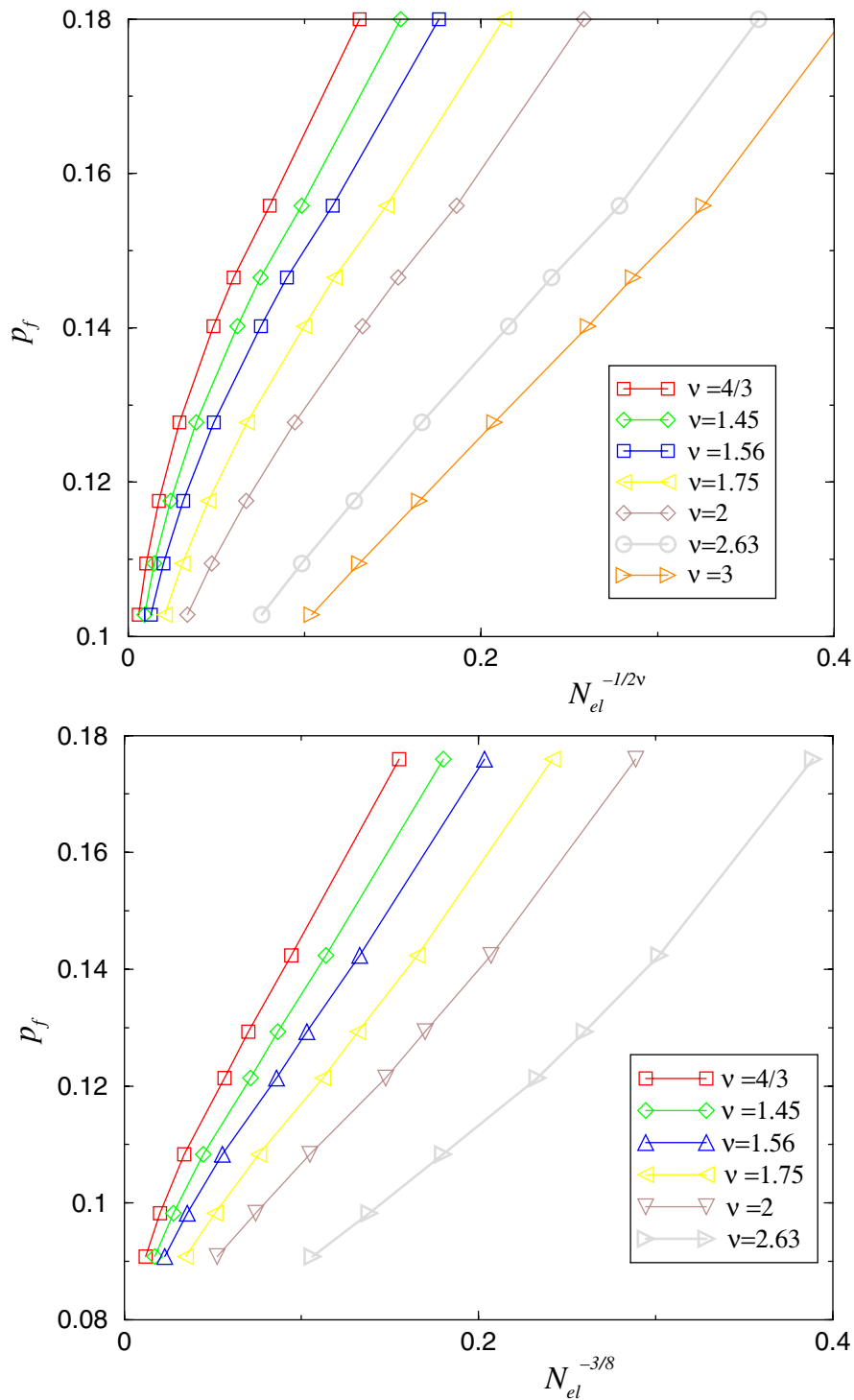


Figure 3. The mean fraction of broken bonds p_f plotted as a function of $N_{el}^{-1/2\nu}$ for the triangular (top) and diamond (bottom) lattices with a uniform threshold distribution. A straight line is observed for different values of ν in each case.

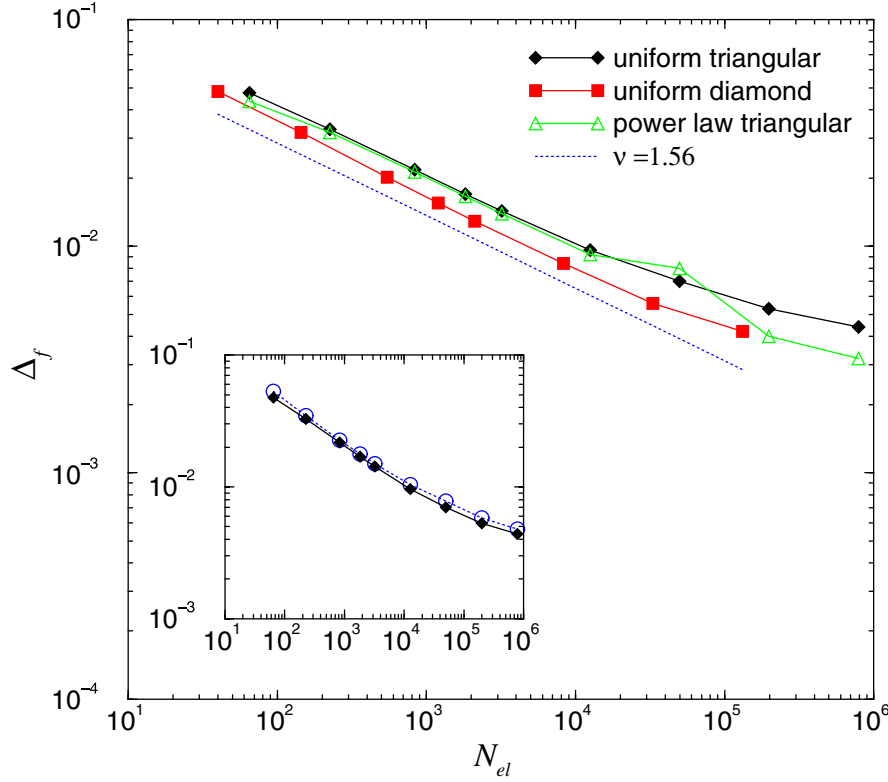


Figure 4. The standard deviation Δ_f of the fraction of broken bonds at failure plotted as a function of N_{el} for different lattices and disorder distributions. The curves are initially described by a power law with exponent -0.32 corresponding to $\nu = 1.56$, but flatten for $L > 100$. In the inset, we compare Δ_f with the same quantity computed at peak load in the case of a triangular lattice with uniform disorder.

For the power law thresholds distributions, such as the one we are using, the scale-invariant thresholds spectrum is given by

$$f_t(\alpha_t) = 2 - \beta\alpha_t \quad \text{where } 0 \leq \alpha_t \leq \frac{2}{\beta} \quad (5)$$

and the two control parameters are $\phi_0 = \beta$ and $\phi_\infty = \infty$ [29, 30]. According to [29, 30], on the basis of the values of these two control parameters, ϕ_0 and ϕ_∞ , the uniform thresholds distributions and the power law thresholds distributions (as long as $\beta < 2$ [30]) belong to the same scaling regime, characterized by diffusive damage and localization (see regime B of figure 18 in [30]). According to this analysis, if the exponent ν were to be universal and in the same universality class as that of uncorrelated percolation, as conjectured in [24], then we expect to find $\nu = 4/3$ for uniform and power law threshold distributions.

4. Damage and percolation

In the case of strong disorder, in the initial stages of damage evolution, bond breaking events occur in an uncorrelated manner and thus resemble percolation. As the damage

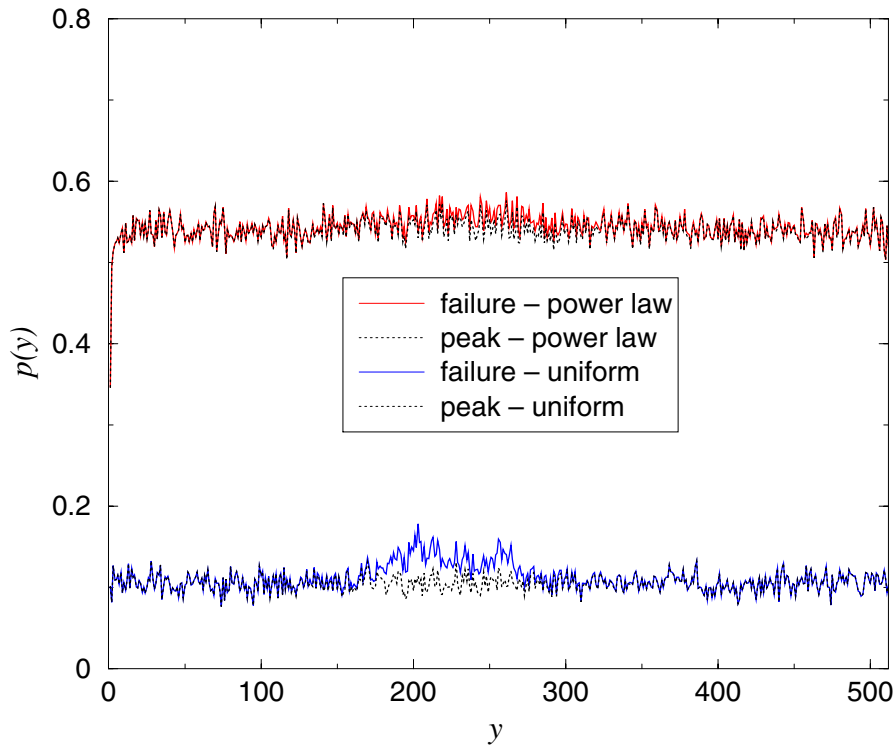


Figure 5. The normalized damage profile $p(y) = n_b(y)/(3L + 1)$ at failure and at peak load in a typical triangular lattice simulation of size $L = 512$ for the cases of uniform and power law disorders. $n_b(y)$ denotes the number of broken bonds in the y th section.

starts to accumulate, some degree of correlation can be expected because of the current enhancement present at the crack tips. A natural question to ask concerns the relevance of these correlations as failure is approached. If correlations are irrelevant one should observe percolation scaling up to failure, as in the case of infinite disorder. On the other hand, in the weak disorder case, the current enhancement at the crack tips is so strong that a spanning crack is nucleated soon after a few bonds are broken (or even after a single bond is broken) [17]. The interesting situation corresponds to the diffuse damage and localization regime, where a substantial amount of damage is accumulated prior to failure. In this regime one should test whether damage follows percolation scaling up to failure.

Hansen and Schmittbuhl [24] have considered broad threshold distributions $p(t) \propto t^{-1+\beta}$, $0 \leq t \leq 1$, with two different values of β , $1/10$ and $1/3$, to see whether percolation scaling was observed for $\beta > 0$. On the basis of the similarities with percolation, they [24] suggested the following finite size scaling law for the fraction of broken bonds:

$$p_f - p_c \sim L^{-(1/\nu)}. \quad (6)$$

In the equation (6), p_f and p_c represent the fracture thresholds for lattice system sizes of L and infinity, respectively. As the system size $L \rightarrow \infty$, the broken bonds at failure $p_f \rightarrow p_c$. The correlation critical exponent ν was found in [24] to be consistent with the percolation

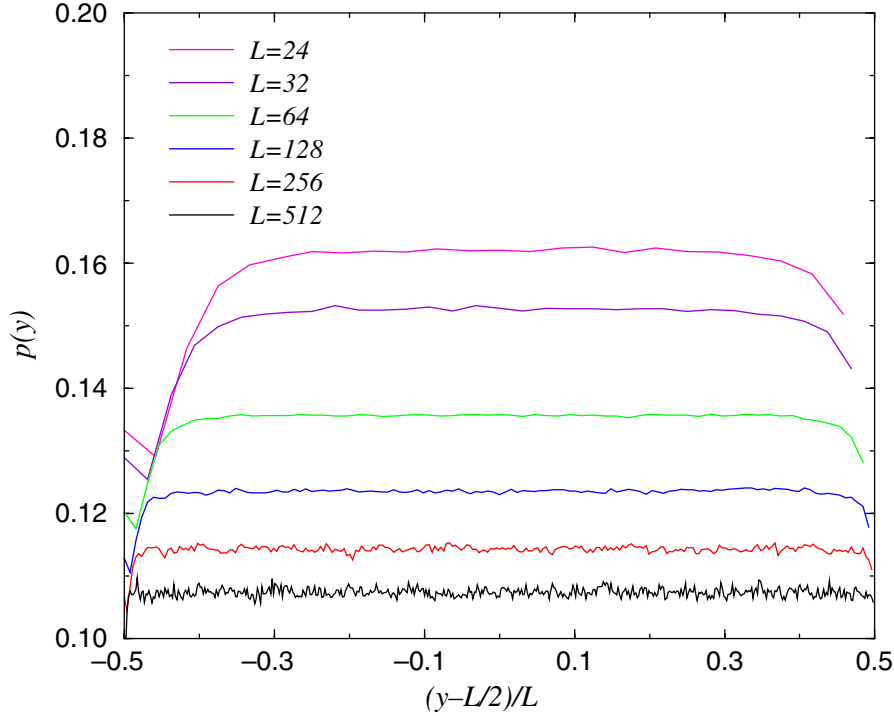


Figure 6. Average damage profiles at peak load obtained by first centring the data around the centre of mass of the damage and then averaging over different samples. The data correspond to uniformly distributed disorder.

value $\nu = 4/3$. An additional test is provided by the damage standard deviation at failure Δ_f [27] which should scale as

$$\Delta_f \sim L^{-(1/\nu)}. \quad (7)$$

Here we test these scaling laws for a wider finite size range than in [24], wherein simulations with sizes up to $L = 60$ are reported. The fraction of broken bonds for each of the lattice system sizes is obtained by dividing the number of broken bonds by the total number of bonds, N_{el} , present in the fully intact lattice system. For triangular lattice topology $N_{el} = (3L + 1)(L + 1)$ and for diamond lattice topology $N_{el} = 2L(L + 1)$. The lattice system sizes considered in this work are $L = \{8, 16, 24, 32, 64, 128, 256, 512\}$. However, since corrections to the scaling laws are strongest for small lattice systems, in the following we use lattice sizes $L \geq 16$ for obtaining the scaling exponents. Table 1 presents mean and standard deviations in the broken bond density (fraction of broken bonds) at the peak load and at failure for various lattice system sizes in both the triangular and diamond lattice systems for the uniform thresholds distribution. In order to compare diamond and triangular lattice topologies, we find it more convenient to use N_{el} rather than L as a finite size parameter. This is because the two lattices have different dependences of the real lattice size (i.e., N_{el}) on the linear size L . We plot in figure 1 the mean fraction of broken bonds at failure p_f as a function of $N_{el}^{-3/8}$ for diamond and triangular lattices, which in principle should obey equation (6) as well. While to accept the percolation hypothesis one should observe a linear regime, a net curvature is apparent in the data especially for sizes $L > 100$. A similar curvature is found in the 50% survival probability p_s .

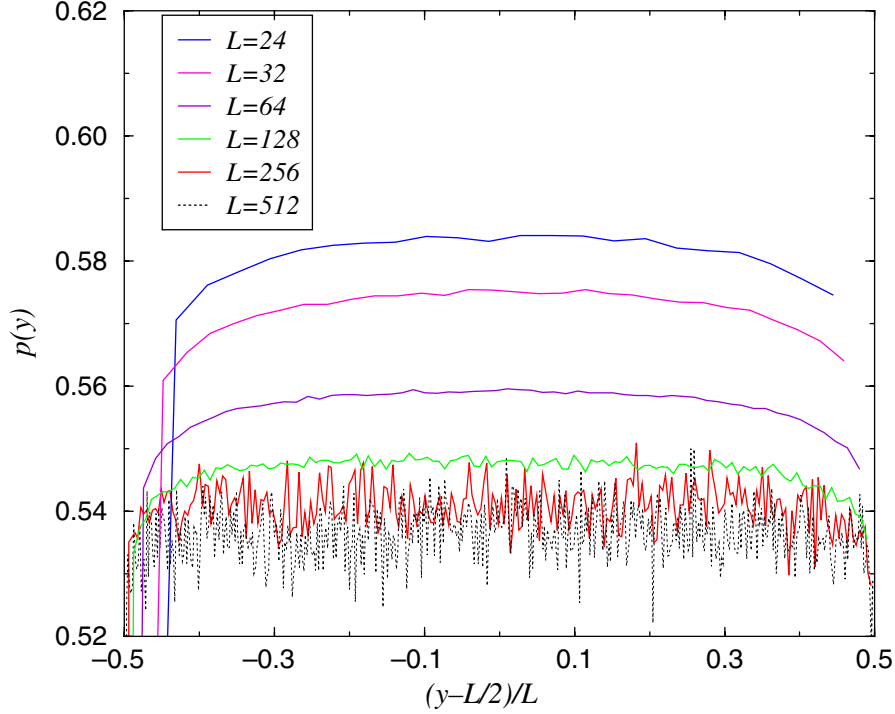


Figure 7. Average damage profiles at peak load obtained by first centring the data around the centre of mass of the damage and then averaging over different samples. The data correspond to power law distributed disorder.

We repeated the same analysis using the power law threshold distribution with $\beta = 1/20$ for triangular lattices of sizes $L = 8, 16, 24, 32, 64, 128, 256, 512$. Table 2 presents means and standard deviations of the broken bond density (fraction of broken bonds) at the peak load and at failure for the power law thresholds distribution. The result is reported in figure 2, and is once again in contrast with percolation scaling (i.e. $\nu \neq 4/3$).

Thus we can conclude that in the random fuse model with uniform and power law distributions, ν is not equal to $4/3$. On the basis of the results, however, we cannot exclude the possibility that equation (6) is valid with a different value of ν . This would correspond to some sort of correlated percolation, which, being a second-order critical phenomenon, is expected to be universal with respect to the lattice structure. A way to test this idea is to plot the data as in figures 1 and 2 using a different value of ν . In figures 3(a) and (b) we report similar plots for the triangular and diamond lattice topologies with the uniform thresholds distribution; it can be seen that a straight line is obtained only for large values of ν . In addition, the ν values for which a straight line is obtained in figures 3(a) and (b) are quite different from one another. For example, a direct fit of the data for $L \geq 16$ yields

$$p_f - 0.0816 = 0.42N_{\text{el}}^{-0.19} \quad (8)$$

for triangular lattices and

$$p_f - 0.0751 = 0.57N_{\text{el}}^{-0.25} \quad (9)$$

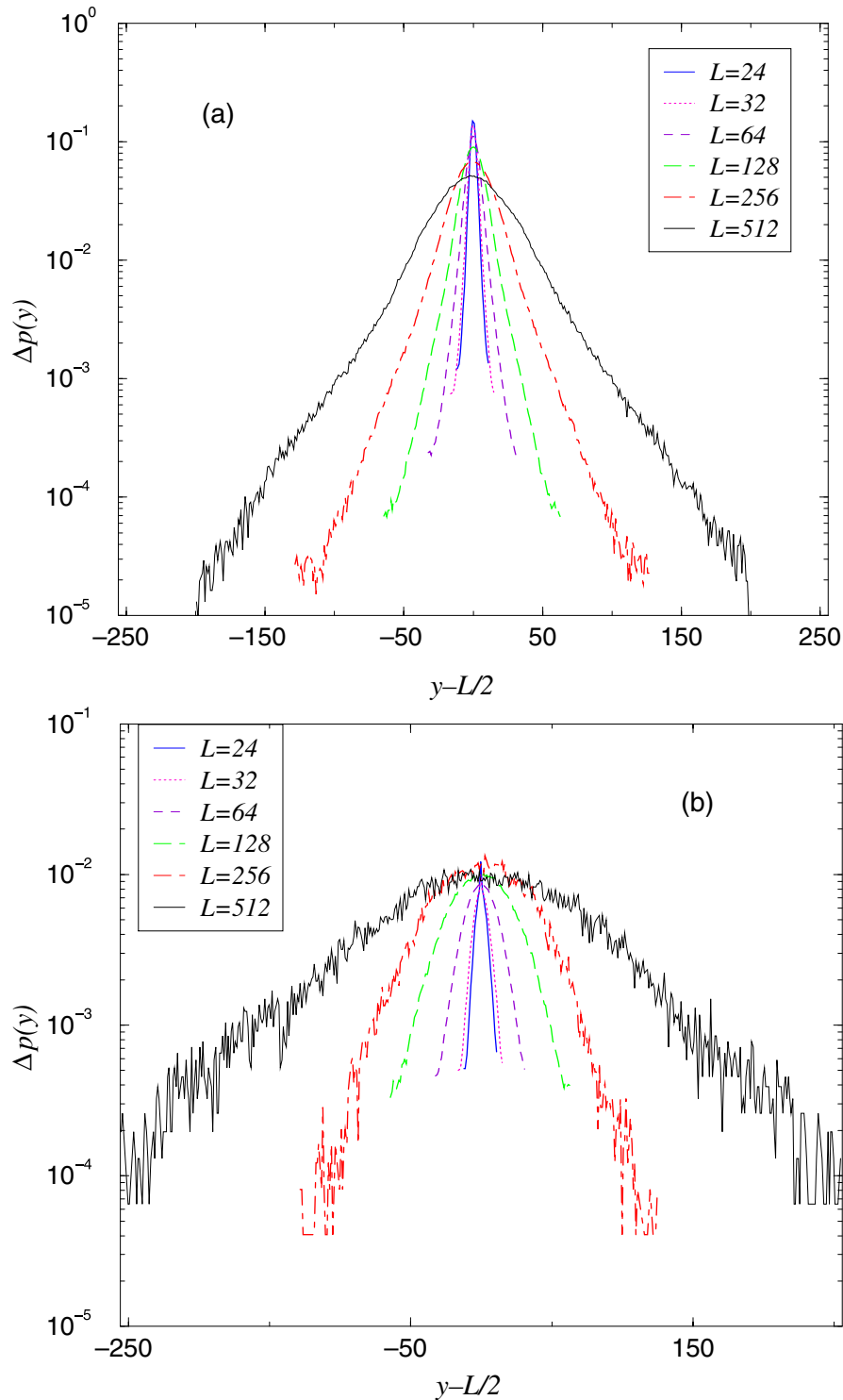


Figure 8. Average profiles for the damage accumulated between peak load and failure. The averaging was performed after shifting the centre of mass. The profiles show exponential tails: (a) uniform disorder, (b) power law disorder.

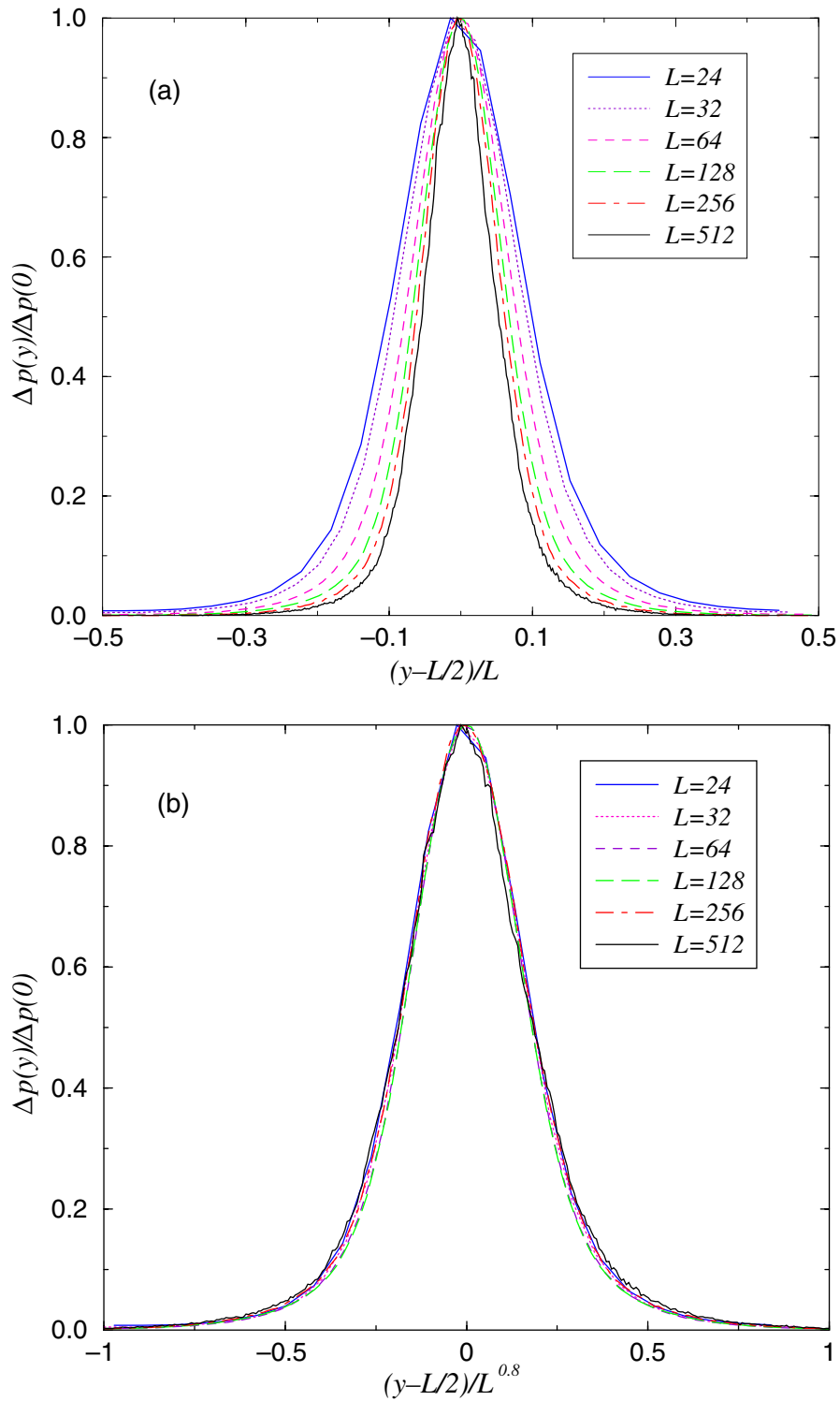


Figure 9. Data collapse of the profiles reported in figure 8(a). (a) Data collapse using a linear scaling for the localization length. (b) Data collapse using a power law scaling.

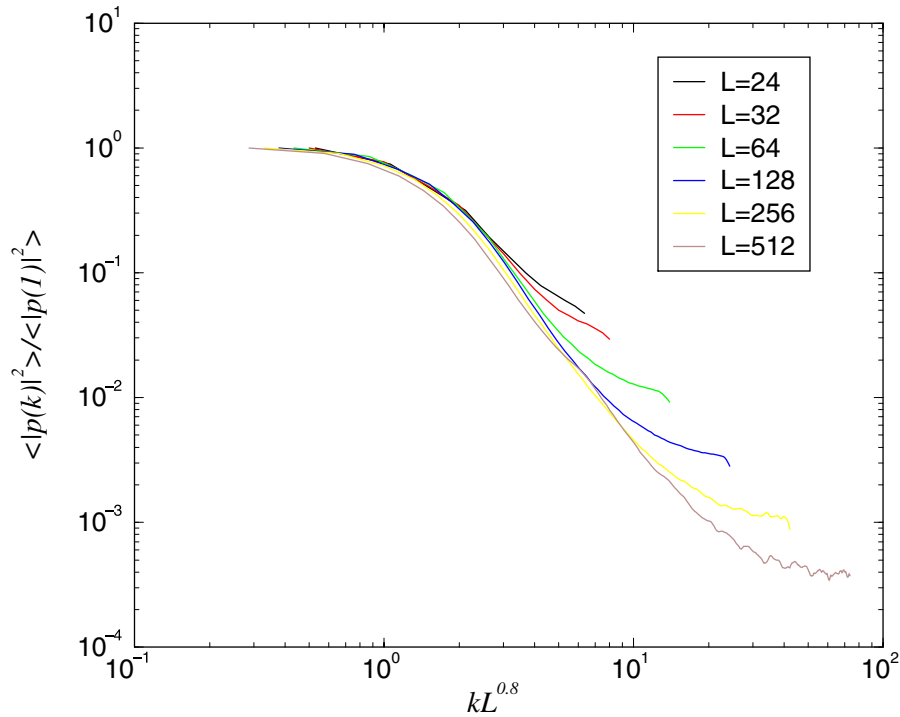


Figure 10. Collapse of the power spectra of damage profiles for uniform disorder.

for diamond lattices. Hence, equations (8) and (9) for triangular and diamond lattice topologies estimate the scaling exponent ν to be equal to 2.63 and 2.0, respectively.

An additional test is provided by plotting the standard deviation of bonds at failure, which in the case of percolation should follow equation (7). For small lattice sizes the data follow a power law with an exponent $\nu \simeq 1.56$, but deviations occur at large sizes. In the framework proposed in [24] one could interpret the data in figure 4 as an indication of an initial correlated percolation process with $\nu = 1.56$, which then crosses over to a localized state where scaling is obscured by the presence of a damage concentration profile. We will show in the next section, however, that there is apparently no localization at peak load (i.e. the maximum current before catastrophic failure). On the other hand, the damage standard deviation at peak load follows closely the behaviour at failure as shown in the inset of figure 4. Thus the damage profile does not appear to be responsible for the deviation from scaling. A different explanation would be that there is no scaling just because the lattice fails abruptly far from a (correlated) percolation critical point.

5. Damage localization

As discussed in the previous section, damage is not described by percolation critical scaling up to the largest sizes. Fracture is abrupt and damage localizes. Here we clarify when and how localization takes place. In particular, we will consider the damage accumulated up to the peak load (i.e. the highest current that the lattice can bear without breaking) and after the peak load up to failure.

In figure 5 we display the damage profile $p(y)$ at failure and at peak load in a single simulation, for the cases of uniform and power law disorders. For uniformly distributed

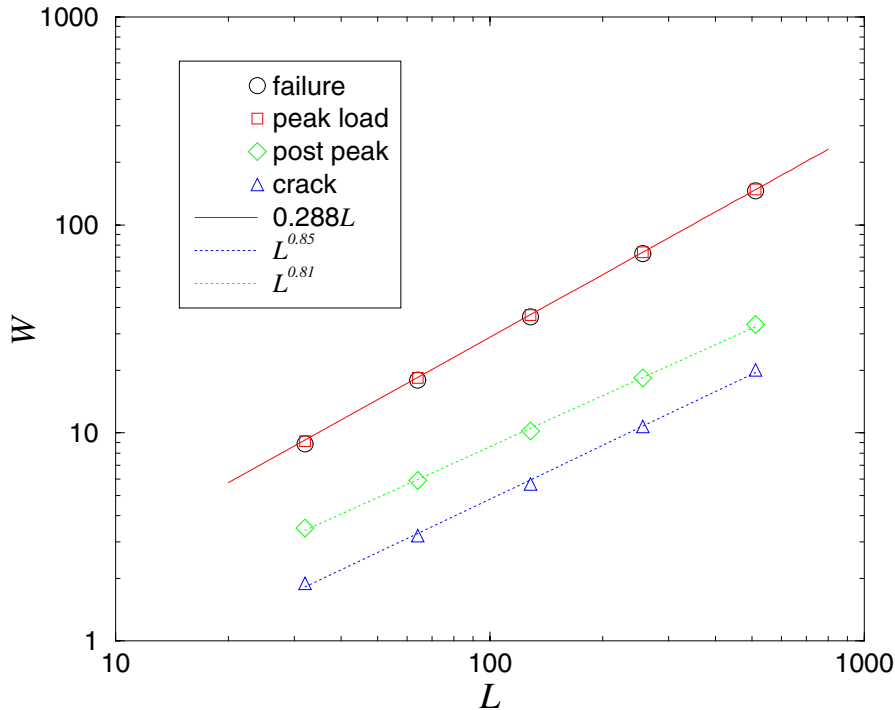


Figure 11. The damage width at peak load and at failure are basically the same. The linear scaling is expected for a uniform distribution and it is not due to localization. On the other hand, localization can be observed for post-peak damage; the width scales as a power law similar to the one observed for the final crack.

thresholds, localization appears clearly at failure, while at peak load the damage spreads homogeneously through the lattice. For power law disorder, it is difficult to assess from these curves the extent of the localization. To obtain a quantitative description of the localization process it is necessary to average over different realizations.

Averaging the profiles is a delicate task since localization does not necessarily take place in the centre, but can in principle occur anywhere along the length of the lattice. Thus one cannot perform a simple average because this would yield a flat average profile irrespective of the individual profile shapes in a single realization. The authors of [26] proposed first shifting the profiles so that they are centred around the maximum and then averaging. This method emphasizes the noise too much, yielding a spurious cusp in the centre. Another possibility is to shift instead by the centre of mass of the damage or, to avoid any effects due to shifting, one can use the Fourier method.

We first consider the damage accumulated up to peak load, shifting the data by the centre of mass method. The result displayed in figure 6 for the uniform disorder distribution clearly shows that there is no localization at peak load. In the case of power law disorder the profile as presented in figure 7 is not completely flat for small scales, but flattens more and more as the size is increased. We tend thus to attribute the apparent profile to size effects. These data imply that the localization profiles already observed in the literature [24]–[26] reflect mostly the final breakdown event, after the

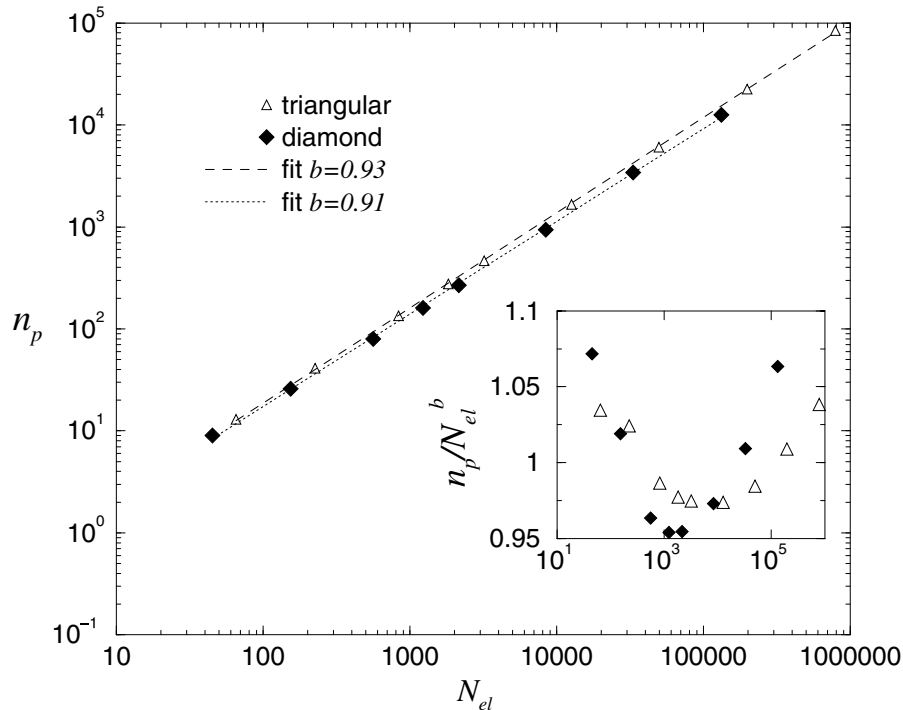


Figure 12. Scaling of the number of broken bonds at peak load for triangular and diamond lattices. The scaling exponents are very close to each other and the difference could be attributed to small size effects. There are, apparently, some systematic errors, as shown in the inset.

final spanning crack is nucleated. To quantify the corresponding damage localization, we can then average the profiles $\Delta p(y)$ obtained considering only the damage accumulated between the peak load and failure. In addition, this procedure considerably reduces the background noise.

The centre of mass shifted averaged profiles for various system sizes are reported in figures 8(a) and (b) for uniform and power law disorder cases and these profiles show that the profile shapes decay exponentially at large system sizes. The damage peak $\langle \Delta p(0) \rangle$ scales as $L^{-0.3}$ for the uniform distribution and is roughly constant for the power law distribution. We have tried different ways to collapse these profiles to extract a localization length. The simple linear scaling $\langle \Delta p(y, L) \rangle / \langle \Delta p(0) \rangle = f((y - L/2)/L)$, proposed in [24], does not yield a very good collapse (see figure 9(a)). A perfect collapse is instead obtained using the form

$$\langle \Delta p(y, L) \rangle / \langle \Delta p(0) \rangle = f(|y - L/2|/\xi) \quad (10)$$

where $\langle \Delta p(0) \rangle = L^{-0.3}$ and $\xi \sim L^\alpha$, with $\alpha = 0.8$ (see figure 9(b)). The situation for power law disorder is similar, but the scaling is less precise. As shown in figure 8(b), the profiles are decaying again exponentially. We could not, however, perform a reliable collapse: a linear scaling seems appropriate for system sizes $L < 256$ but fails for larger sizes.

To obtain additional confirmation of these results, we perform a Fourier analysis of the Δp profiles, thus avoiding any possible bias due to the shifting. We first compute the

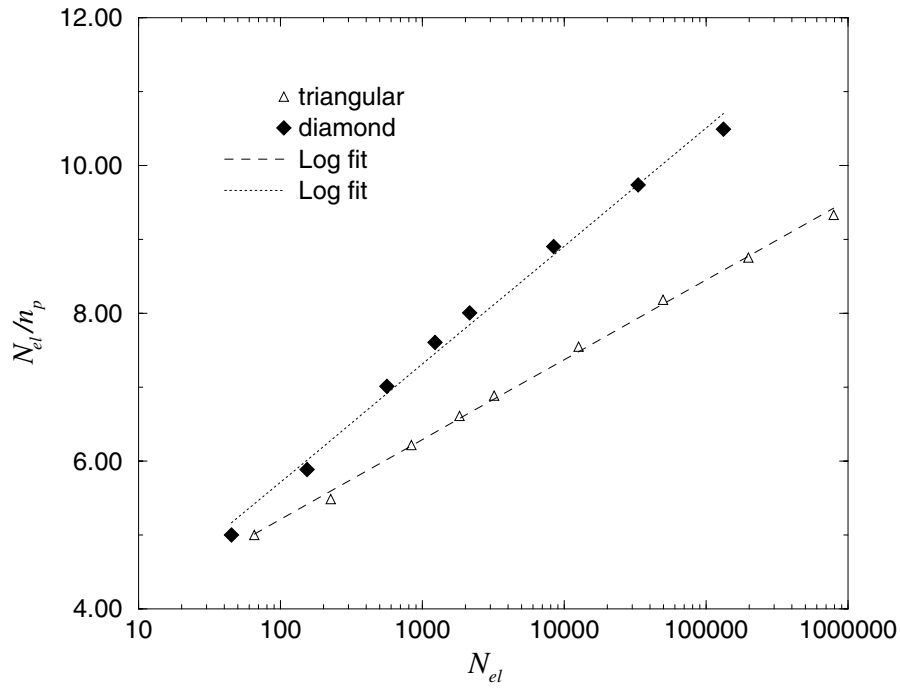


Figure 13. The number of broken bonds at peak load can also be fitted by a linear function times a logarithmic correction by plotting n_p/N_{el} as a function of N_{el} in a log-linear plot.

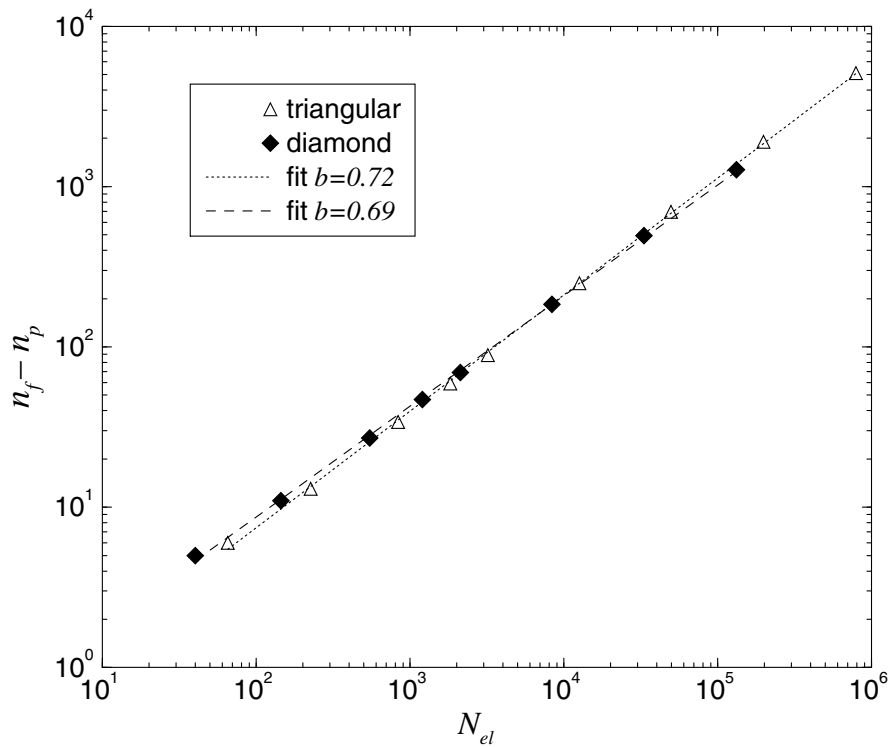


Figure 14. The number of bonds broken in the last catastrophic event scales as a power law of N_{el} .

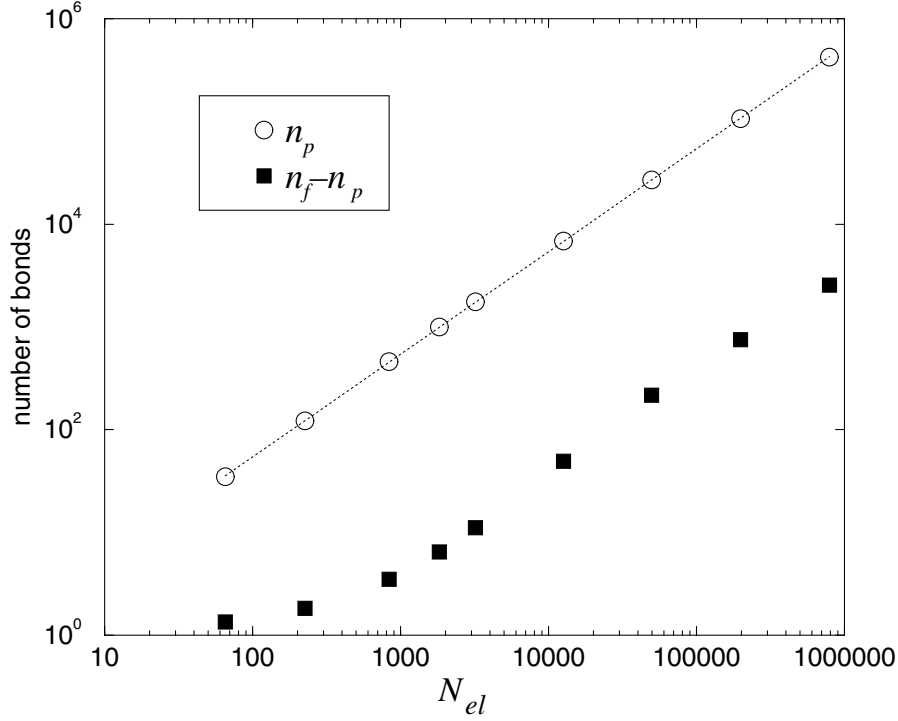


Figure 15. The scaling of the number of broken bonds for a triangular lattice with the power law threshold distribution. The scaling exponent for n_p is very close to one and a similar result seems to hold asymptotically for $n_f - n_p$.

magnitude of the Fourier transform for each realization and then average over disorder. From equation (10) we would expect the power spectrum of the profile to follow

$$\langle |\tilde{p}(k)|^2 \rangle / \langle |\tilde{p}(1)|^2 \rangle = \tilde{f}(kL^{0.8}). \quad (11)$$

This result applies to an infinite system, and finite size deviations and other problems of the discrete Fourier transform are expected to affect the data. Nonetheless, as shown in figure 10, we can collapse the curves reasonably well using the same exponent as in real space.

It is also possible to estimate the localization length directly, independently of the profile averaging. This is done by computing the width of the damage cloud as $W \equiv (\langle (y_b - \bar{y}_b)^2 \rangle)^{1/2}$, where y_b is the y coordinate of a broken bond and the average is taken over different realizations. We have first measured W at peak load and at failure, and obtained a result $W \sim L$, consistent with earlier results [29] (see figure 11). This result is expected, since for uniformly distributed damage such as at the peak load, $W \simeq L/\sqrt{12} \sim 0.288L$, and this is in excellent agreement with the numerical data. This is consistent with the fact that there is no localization at peak load, and at failure the damage cloud is dominated by the uniform fluctuations already present at peak load. Any additional scaling due to localization is obscured. To uncover it we can restrict the averaging to just the bonds broken in the last failure event (post-peak damage), obtaining $W \sim L^{0.81}$ which is consistent with the data collapse of the profiles. It is interesting to note that the width of the final crack scales as well with a similar exponent. This supports

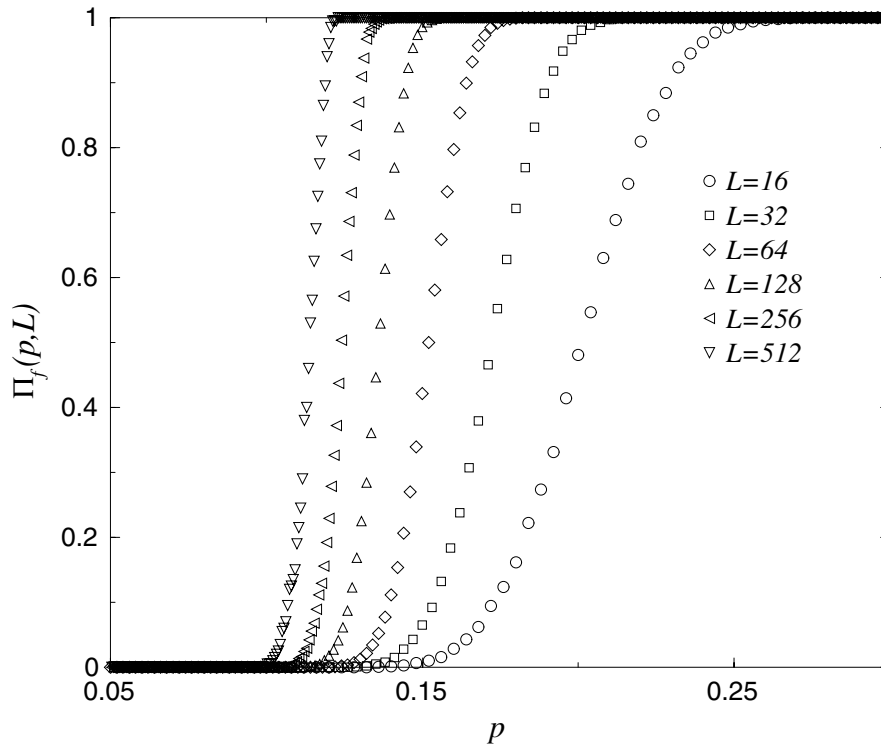


Figure 16. The cumulative probability distribution for the fraction of broken bonds at failure for triangular lattices of different system sizes.

the idea that localization is produced by catastrophic failure which yields at the same time the crack and the damage profile.

6. Scaling of the damage density

It has been noted in the previous section that the final breakdown event is very different from the initial precursors. Thus, we consider the scaling of the number of broken bonds at the peak load, n_p , that excludes the last catastrophic event. In figure 12 we plot n_p as a function of the lattice size N_{el} for triangular and diamond lattices. The data display a reasonable power law behaviour $n_p \sim N_{el}^b$, with $b = 0.93$ and 0.91 for triangular and diamond lattices, respectively, as previously shown in [18]. Thus the difference between the two lattices is marginal and may be attributed to the results obtained from the smaller lattice sizes, where corrections to the fractal scaling may exist. By plotting n_p/N_{el}^b versus N_{el} (see the inset of figure 12) we show that some systematic deviations appear. The data could be equally well fitted by a linear law times a logarithmic correction $n_p \simeq N_{el}/\log(N_{el})$, as suggested in [26] (see figure 13). Both of these fits imply that in the limit of large lattices the fraction of broken bonds prior to fracture vanishes (i.e. $p_c = 0$ in the thermodynamic limit).

Figure 14 presents the scaling for the number of broken bonds, $(n_f - n_p)$, after crossing the peak load. Once again, the scaling exponents for $(n_f - n_p)$ are similar for the triangular and diamond lattice topologies, and equal to 0.72 and 0.69 respectively. These exponents

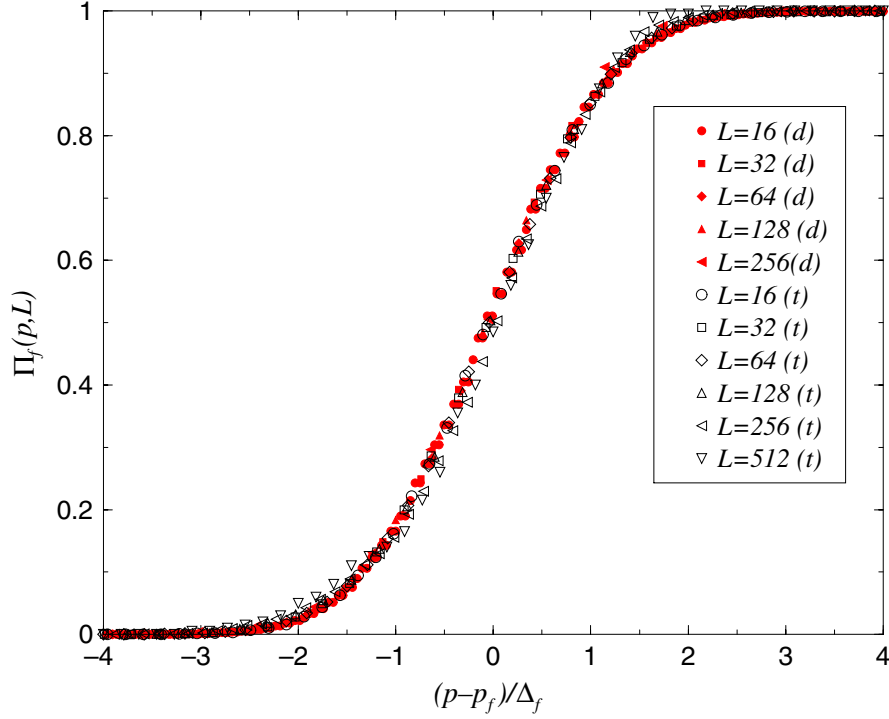


Figure 17. The collapsed cumulative failure probability distributions for both triangular (t) and diamond (d) lattices of different system sizes with uniform disorder when plotted as a function of the reduced variable $\bar{p}_f = (p - p_f)/\Delta_f$.

are consistent with the parameters estimated from the profile $(n_f - n_p) \sim \langle p(0) \rangle (3L+1)\xi \sim L^{1.5}$. The behaviour of power law disorder appears to be simpler. The number of broken bonds at peak load scales linearly with N_{el} , as shown in figure 15. A similar result holds asymptotically for $(n_f - n_p)$ (see figure 15), which is again consistent with the profile scaling.

7. The failure probability distribution

The cumulative probability distribution for the fraction of broken bonds at failure (also termed the cumulative failure probability distribution), defined as the probability $\Pi_f(p_b, L)$ that a system of size L fails when the fraction of broken bonds equals $p_b = n_b/N_{el}$, where n_b is the number of broken bonds, is plotted in figure 16 for varying triangular lattice system size. In [24] a data collapse of a different but related distribution (i.e., the survival probability) was attempted using percolation scaling. As is evident from the failure of such a scaling (i.e., equation (6)), this collapse is poor.

On the other hand, we obtain a very good collapse by simply plotting the distribution in terms of $\bar{p}_f \equiv (n_b - \mu_{n_f})/\sigma_{n_f} = (p_b - p_f)/\Delta_{p_f}$, where μ_{n_f} and σ_{n_f} denote the mean and standard deviation of the number of broken bonds at failure, and p_f and Δ_{p_f} denote the mean and standard deviation of the fraction of broken bonds at failure. Figure 17 shows that $\Pi_f(p, L)$ may be expressed in a universal scaling form such that $\Pi_f(p, L) = \Pi_f(\bar{p}_f)$ for both triangular and diamond lattice topologies of different system sizes L . A similar collapse can be performed for the power law disorder distribution (see figure 18). The

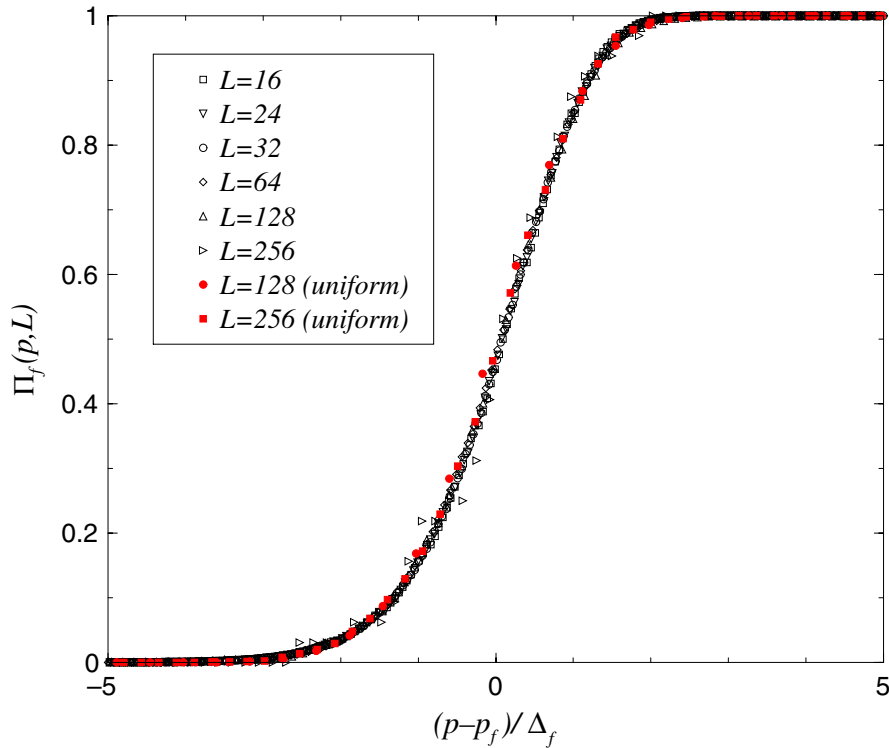


Figure 18. The collapsed cumulative failure probability distributions for lattices of different system sizes with power law disorder when plotted as a function of the reduced variable $\bar{p}_f = (p - p_f) / \Delta_f$. For comparison we also include two curves obtained in the case of uniform disorder.

excellent collapses of the data in figures 17 and 18 suggest that the cumulative failure probability distribution, $\Pi_f(p_b, L) = \Pi_f(\bar{p}_f)$, may be universal in the sense that it is independent of the lattice topology and disorder distribution. We have also checked that the distributions at peak load obey essentially the same laws, i.e., $\Pi(\bar{p}) = \Pi_f(\bar{p}_f) = \Pi_p(\bar{p}_p)$, where $\Pi_p(\bar{p}_p)$ is the probability that a system of size L is at the peak load when the fraction of broken bonds equals p_b , and \bar{p}_p is the corresponding reduced variable at the peak load. Finally, the collapse of the data in figure 19 indicates that a Gaussian distribution adequately describes Π_f .

The fact that damage is Gaussian distributed suggests that there is no divergent correlation length at failure, consistent with the conclusions of [18] that reported a finite correlation length at failure. Long-range correlations in the damage would imply that the central limit theorem does not hold and hence the normal distribution would not be an adequate fit to the data. The absence of long-range correlation is again in agreement with the hypothesis that fracture is analogous to a first-order transition [13].

8. Discussion

This paper presents numerical simulations on large two-dimensional triangular and diamond lattice fuse networks with uniform and power law disorder distributions. We focus our analysis on the statistical properties and localization features of the damage as

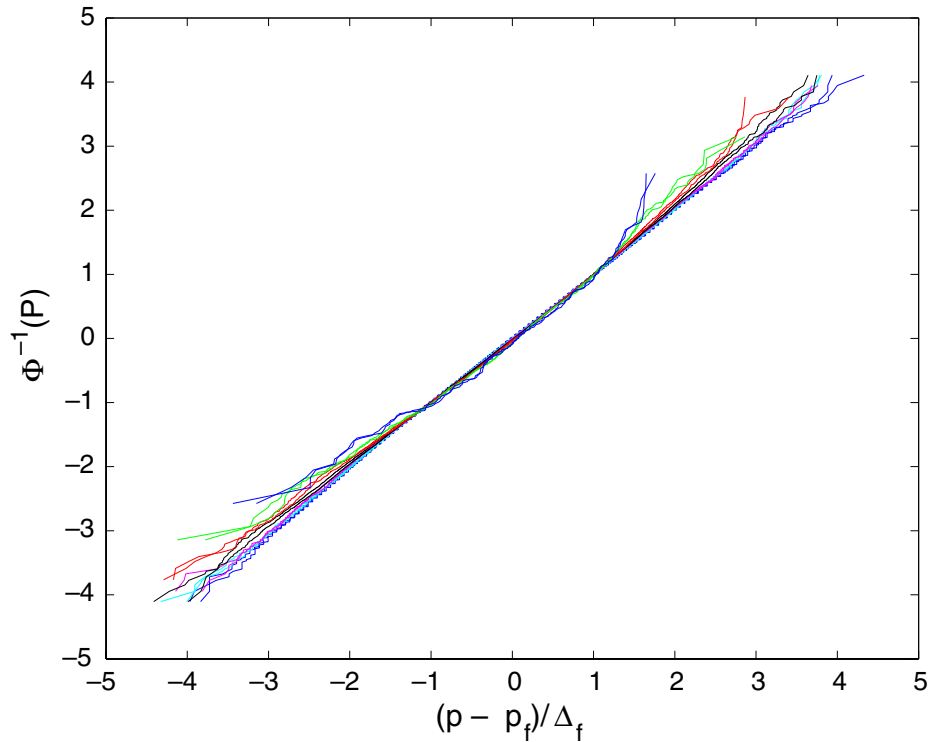


Figure 19. Normal distribution fits for the cumulative probability distributions of the fractions of broken bonds at failure and at the peak load for triangular lattices of different system sizes $L = \{16, 24, 32, 64, 128, 256, 512\}$.

a function of the lattice type, size and disorder form. The use of high statistical sampling and relatively large lattice sizes is essential for obtaining reliable results.

The picture emerging from our analysis is that, for strong disorder, damage accumulates first in the system in an uncorrelated (or short-range correlated) manner. This process continues up to the peak load, where no apparent sign of localization is present. Further increase of the current leads to catastrophic failure through a large avalanche event, whose size scales with the lattice size as $L^{1.45}$. The damage accumulated in this event is localized in a cloud surrounding the final crack. The damage profile has exponential tails and can be collapsed for different system sizes using an appropriate scaling law.

The accumulated damage density at failure p_f appears to be far from a percolation-like critical point, since we could not find a reliable universal scaling law as the system size is varied. A different possibility that we have tested is that $p_f \rightarrow 0$ as $L \rightarrow \infty$, but a fit using simple scaling forms shows some deviation as well. Thus we cannot decide whether p_f decays slowly to zero or to a non-vanishing asymptotic value. This value, however, would not necessarily coincide with a critical point.

Finally, this study also presents the scaling of the cumulative failure probability distribution, which is defined as the probability that a lattice system fails at a given fraction of broken bonds. On the basis of the numerical results presented, we show that the cumulative failure probability distribution is universal in the sense that it does not

depend on the lattice topology, i.e., the distributions are identical for triangular and diamond lattice topologies. Furthermore, a *normal* distribution presents an adequate fit to the data.

Acknowledgments

This research was sponsored by the Mathematical, Information and Computational Sciences Division, Office of Advanced Scientific Computing Research, US Department of Energy, under contract number DE-AC05-00OR22725 with UT-Battelle, LLC. We thank M J Alava, A Hansen, H J Herrmann and S Roux for useful remarks and discussions.

References

- [1] Herrmann H J and Roux S (ed), 1990 *Statistical Models for the Fracture of Disordered Media* (Amsterdam: North-Holland)
- Bardhan K K, Chakrabarti B K and Hansen A (ed), 1994 *Non-Linearity and Breakdown in Soft Condensed Matter* (Berlin: Springer)
- Chakrabarti B K and Benguigui L G, 1997 *Statistical Physics of Fracture and Breakdown in Disordered Systems* (Oxford: Oxford University Press)
- Krajcinovic D and van Mier J G M, 2000 *Damage and Fracture of Disordered Materials* (New York: Springer)
- [2] Mandelbrot B B, Passoja D E and Paullay A J, 1984 *Nature* **308** 721
- [3] For a review see, Bouchaud E, 1997 *J. Phys.: Condens. Matter* **9** 4319
- [4] Garcimartín A, Guarino A, Bellon L and Ciliberto S, 1997 *Phys. Rev. Lett.* **79** 3202
- Guarino A, Garcimartín A and Ciliberto S, 1998 *Eur. Phys. J. B* **6** 13
- [5] Maes C, Van Moffaert A, Frederix H and Strauven H, 1998 *Phys. Rev. B* **57** 4987
- [6] Petri A, Paparo G, Vespignani A, Alippi A and Costantini M, 1994 *Phys. Rev. Lett.* **73** 3423
- [7] Salminen L I, Tolvanen A I and Alava M J, 2002 *Phys. Rev. Lett.* **89** 185503
- [8] Hansen A, Hinrichsen E L and Roux S, 1991 *Phys. Rev. Lett.* **66** 2476
- [9] Batrouni G G and Hansen A, 1998 *Phys. Rev. Lett.* **80** 325
- [10] Räisänen V I, Seppälä E T, Alava M J and Duxbury P M, 1998 *Phys. Rev. Lett.* **80** 329
- [11] Seppälä E T, Räisänen V I and Alava M J, 2000 *Phys. Rev. E* **61** 6312
- [12] Hansen A and Hemmer P C, 1994 *Phys. Lett. A* **184** 394
- [13] Zapperi S, Ray P, Stanley H E and Vespignani A, 1997 *Phys. Rev. Lett.* **78** 1408
- Zapperi S, Ray P, Stanley H E and Vespignani A, 1999 *Phys. Rev. E* **59** 5049
- [14] Zapperi S, Vespignani A and Stanley H E, 1997 *Nature* **388** 658
- [15] Caldarelli G, Di Tolla F G and Petri A, 1996 *Phys. Rev. Lett.* **77** 2503
- [16] Räisänen V I, Alava M J and Nieminen R M, 1998 *Phys. Rev. B* **58** 14288
- [17] Kahng B, Batrouni G G, Redner S, de Arcangelis L and Herrmann H J, 1988 *Phys. Rev. B* **37** 7625
- [18] Delaplace A, Pijaudier-Cabot G and Roux S, 1996 *J. Mech. Phys. Solids* **44** 99
- [19] de Arcangelis L, Hansen A, Herrmann H J and Roux S, 1989 *Phys. Rev. B* **40** 877
- [20] Nukala P K V V and Simunovic S, 2003 *J. Phys. A: Math. Gen.* **36** 11403
- [21] de Arcangelis L, Redner S and Herrmann H J, 1985 *J. Physique Lett.* **46** 585
- Sahimi M and Goddard J D, 1986 *Phys. Rev. B* **33** 7848
- [22] Andersen J V, Sornette D and Leung K T, 1997 *Phys. Rev. Lett.* **78** 2140
- Sornette D and Andersen J V, 1998 *Eur. Phys. J. B* **1** 353
- Johansen A and Sornette D, 2000 *Eur. Phys. J. B* **18** 163
- [23] Roux S, Hansen A, Herrmann H J and Guyon E, 1988 *J. Stat. Phys.* **52** 237
- [24] Hansen A and Schmittbuhl J, 2003 *Phys. Rev. Lett.* **90** 45504
- [25] Bakke J O H, Bjelland J, Ramstad T, Stranden T, Hansen A and Schmittbuhl J, 2003 *Phys. Scr. T* **106** 65
- [26] Reurings F and Alava M J, 2004 *Preprint cond-mat/0401592*
- [27] Ramstad T *et al.*, 2003 *Preprint cond-mat/0311606*
- [28] Batrouni G G, Hansen A and Nelkin M, 1986 *Phys. Rev. Lett.* **57** 1336
- Batrouni G G, Hansen A and Nelkin M, 1988 *J. Stat. Phys.* **52** 747
- [29] Hansen A, Hinrichsen E L and Roux S, 1991 *Phys. Rev. B* **43** 665
- [30] Hansen A and Roux S, *Statistical toolbox for damage and fracture*, 2000 *Damage and Fracture of Disordered Materials* ed D Krajcinovic and J G M van Mier (New York: Springer) pp 17–101